Experimental Investigation of Welded Steel T-Stub Components Under Different Loading Rates

Grace Kendall[1], Artem Belyi[2] and Ahmed Elkady[3*]

[1]Department of Civil, Maritime and Environmental Engineering, University of Southampton, United Kingdom. Address: Burgess road, Boldrewood campus, Southampton SO17 7QF, UK. e-mail: gck1g21@soton.ac.uk

[2]Department of Civil, Maritime and Environmental Engineering, University of Southampton, United Kingdom. Address: Burgess road, Boldrewood campus, Southampton SO17 7QF, UK. e-mail: ab1u20@soton.ac.uk

[3]Department of Civil, Maritime and Environmental Engineering, University of Southampton, United Kingdom (*corresponding author*). Address: Burgess road, Boldrewood campus, Southampton SO17 7QF, UK. e-mail: a.elkady@soton.ac.u

Abstract

The equivalent steel T-stub approach is widely used in practice to analyse and design bolted steel joints that are otherwise complex to study. The available analytical and empirical models for characterizing the response of T-stub components are based on numerous experimental and numerical research studies. This research is mostly concerned with the pseudo-static response of the T-stub. However, natural and man-made hazards (such as earthquakes and impacts) are dynamic. Considering the strain-rate sensitivity of steel, dynamic effects may have a notable effect on structural behaviour. A limited number of studies investigated the response of steel components/joints at high loading rates with inconclusive, and sometimes conflicting, observations. Accordingly, an experimental study is undertaken to address the data shortage. A total of 57 welded steel T-stubs were tested under monotonic tension. The main test parameters included the T-stub flange plate thickness, the loading rate, and the bolt preload condition.

The test data underscored the influence of the loading rate and bolt preload. Notably, at a loading rate of 50mm/sec, an average of 35% reduction in the elastic stiffness, a 10% amplification of strength, and a 22% reduction in ductility is observed compared to the reference pseudo-static loading rate. The paper discusses the test observations in detail, evaluates the findings considering past research, and assesses potential implications on design.

Keywords: Steel T-stub, Strain rate, Loading rate, Connection ductility, Bolt preload

Introduction

The current design paradigm relies on tuning the relative strength and stiffness of the different joint and connection components (column, beam, endplate, angle cleat, bolts, and welds) to achieve the target rigidity, maintain a hierarchal –ductile- progression of damage, and avoid early brittle failure modes (e.g., weld failure and bolt rupture). To study bolted steel connections and particularly semi-rigid ones, the connection is discretised into an assembly of T-stub components. This is illustrated in Figure 1 which shows a few equivalent T-stubs extracted from common bolted steel connections. Steel T-stubs can be divided into two main categories: welded and hot-rolled. Welded T-stubs represent components such as the beam to endplate components while hot-rolled T-stubs represent components such as the column flange and angle cleats. Understanding, and consequently accurately predicting, the behaviour of steel T-stubs is fundamental in computing the stiffness, strength and ductility of steel joints, as part of the analytical and mechanical methodologies [1].

Current analytical and empirical methods for characterizing the mechanical response parameters of steel T-stubs under tension are based on decades of numerous experimental research studies. These studies mostly involved pseudo-static loading conditions, where displacements/forces are applied at a very low rate (typical loading speed less than 1mm/s or a strain rate less than 10^{-3} s^{-1}). Although pseudo-static tests are convenient, they are not a true representation of real hazards (earthquakes, collisions, explosions, column loss, etc.) which are dynamic. These dynamic hazards exert inertia loads on structures, amplify

the shear force demands in structural members and components and accentuate the material's strain rate ($\dot{\varepsilon}$) sensitivity. For the latter, steel is a particularly strain-rate sensitive construction material, where high strain rates can amplify the yield and ultimate stress by up to 50% and 20%, respectively [2-5]. Most critically, a reduction in fracture strain and fracture toughness (i.e., material ductility) of up to 50% is observed, particularly in high-strength steel grades, which increases the risk of bolt and weld failure [6-9].

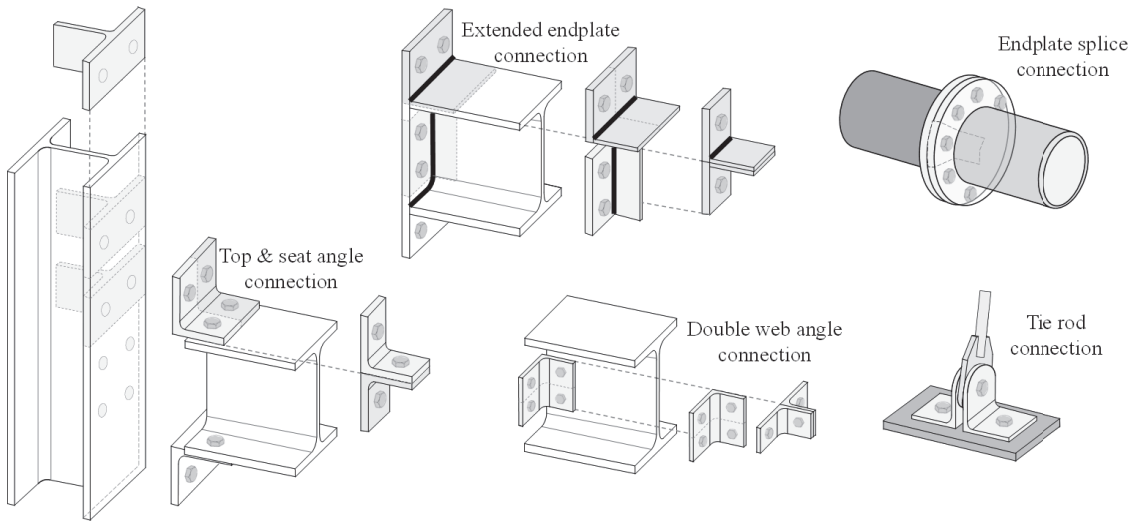

Fig. 1. T-stub components in commonly used bolted steel connections.

Concerning bolted joints, dynamic loading may likely trigger connection slippage and induce larger shearing forces on bolts; thereby leading to unfavourable brittle failure modes [10, 11]. This is also dependent on the amount of bolt preload, which controls the connection's ability to resist shear forces through friction and consequently the amount of slippage and the percentage of shear load transfer through the bolt shearing and plate hole bearing [2]. These phenomena can potentially lead to an unfavourable deviation from the failure mode stipulated in the design process. This threatens global structural robustness and can trigger progressive collapse. This issue becomes more critical knowing that several researchers noted that the current design codes and available predictive numerical models, can sometimes be unreliable in predicting the pseudo-static connection response parameters and deformation modes [12, 13]. This may be exacerbated under realistic dynamic loading. For instance, recent tests [14]

showed that the current Eurocode 3 [1] design overpredicts the connection strength by about 30% under high loading rates.

While testing full-scale bolted joints at high loading rates is costly, testing T-stub components is not and can provide equally valuable insights. Nonetheless, while hundreds of T-stubs were tested in the literature, a limited number of those were tested at high loading rates. The findings from these limited tests although useful are not conclusive and sometimes contradictory. Dinu et al. [15] tested welded T-stubs under loading rates ranging from 0.05 to 10 mm/s. They noted a small influence of the loading rate on the ultimate capacity, ductility, and failure mode. Baldassino et al. [16] tested welded and hot-rolled T-stubs, with 10mm and 16mm flange plates, at loading rates ranging between 0.07 mm/s and 326 mm/s. The tests also showed limited influence on load capacity and ductility but noted the importance of the weld quality to prevent brittle failures. Relevant test data on bolted lap components in tension and shear noted the increase in strength, reduction in ductility and the significant effect of loading rate on slippage in friction-type connections [2, 15]. Others also reported a 2-6% increase in ultimate loads accompanied by an 8% to 9% increase in ductility [17]. Furthermore, available tests suggest that bolt preload provides significant enhancements in the initial stiffness, increasing it by up to three times compared to snug-tight T-stub connections [18-20]. Zhang et al. [18] further noted that bolt preload significantly enhanced the deformation capacity by 27%. Finally, the limited number of full-scale joints tested under high loading rates showed that under dynamic loading, some specimens experienced an increase in strength/stiffness and reduction in ductility coupled with large shear-to-flexural force ratios, while others had limited strength due to the early onset of bolt thread stripping [14, 21-23]. Relevant tests on welded connections [24-27] reported a 10% to 20% strength amplification but inconclusive observations on ductility.

To complement the existing experimental data in the literature and help draw a clearer understanding, 57 welded T-stub specimens are tested as part of this study. The focus is to investigate both the loading rate and bolt preload effects on the T-stub response. The subsequent sections describe the test parameters, and

the test setup, followed by a discussion of the observed deformation modes and the individual and combined effect of the test parameters on the elastic stiffness, strength, and ductility.

Test Specimens and Parameters

A total of 57 welded T-stub specimens were tested. Table 1 summarizes the geometric parameters of the test specimens. The specimens are labelled using the following notation: **T***x*-*y*, where *x* is the number of bolts and *y* is the flange plate thickness (t_f). Specifically, two main bolt layouts are considered: T2 and T4. T2 involves a single bolt row with two bolt columns layout and T4 involves a two bolt rows by two bolt columns layout, as illustrated in Figure 2. All T-stubs had a flange width (b_f), of 220mm and M16 Grade 8.8 bright zinc-plated steel bolts [28]. The T2 and T4 specimens had a plate length (L_f) equal to 80mm and 150mm, respectively. Referring to Figure 2, most T-stubs had a bolt gauge distance (g) of 120mm and were tested in a T-stub-on-rigid support assembly configuration. Two specimen groups employed variations of the T2-10 specimen. Those involved one group with larger L_f=120mm (labelled as *T2-10-120*) and another with a double T-stub assembly configuration (see Figure 2) and g=180mm (labelled T2-10D). The specimens' geometry differs primarily in terms of t_f which ranges from 6mm to 20mm, and L_f which ranges from 80mm to 150mm. The specimens are subjected to different monotonic tensile loading rates ranging from pseudo-static 0.05mm/sec to dynamic 100mm/sec. The selected loading rates are consistent with those used in the literature which represent the expected rates under gravity-driven progressive collapse scenarios [29]. Two bolt-preload conditions are considered: snug-tight (ST) and full-preloaded (FT).

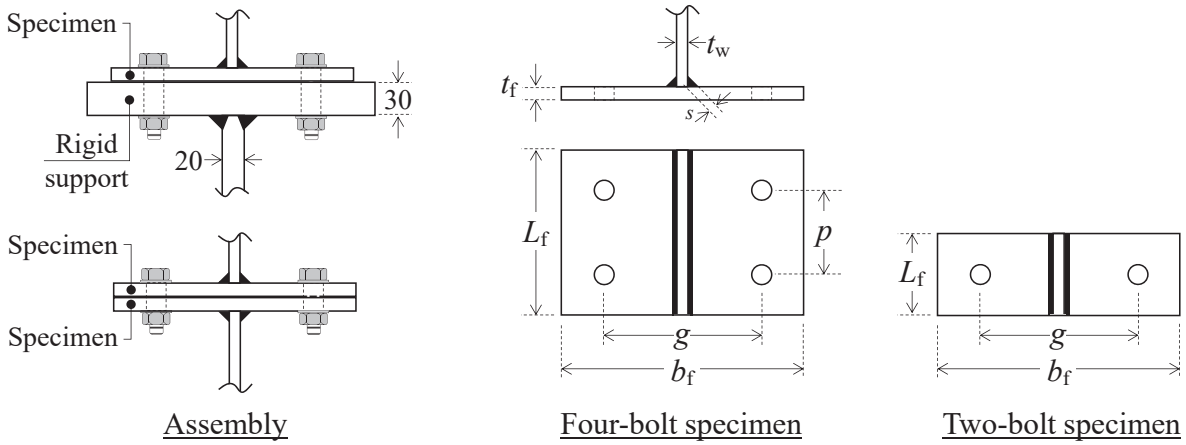

Fig. 2. Schematical diagram of test specimens layout and geometric parameters.

Table 1. Summary of test specimens geometry and loading parameters

No.	ID	Geometry								Preload condition	Loading rate [mm/sec]
		b_f	t_f	L_f	t_w	g	p	s	N_{bolt}		
3	T2-6	220	6	80	10	120	-	5	2	ST	0.05; 10; 50
6	T2-8	220	8	80	10	120	-	5	2	ST; FP	0.05; 20; 50
6	T2-10	220	10	80	10	120	-	5	2	FP	0.05; 10; 20
3	T2-10-120	220	10	120	10	120	-	5	2	ST; FP	0.05; 10; 50
3	T2-10D*	220	10	80	10	180	-	5	2	FP	0.1; 40; 100**
5	T2-12	220	12	80	12	120	-	5	2	FP	0.05; 5; 10; 20; 50
6	T2-15	220	15	80	10	120	-	6	2	ST; FP	0.05; 1; 20; 50
4	T2-16	220	16	80	12	120	-	6	2	FP	0.05; 5; 10; 20
6	T2-20	220	20	80	16	120	-	8	2	ST; FP	0.05; 20; 50
6	T4-8	220	8	150	12	120	90	5	4	ST; FP	0.05;1; 10; 50
9	T4-12	220	12	150	12	120	90	6	4	ST; FP	0.05; 5; 10; 20

* Double T-stub configuration
** The reported speed represents the separation gap speed (i.e., double that of a single T-stub)

All plates are fabricated from grade S275 steel. The material properties are described in the next section. Fillet welding is used to join the web and flange plates. The weld size (s) is summarized in Table 1. Welding was conducted using the TIG process with a 1.6~2.4mm filler wire of grade ER70S-2. During welding, measures were taken to ensure a right angle between the welded plates and to minimize flange

plate distortion, as shown in Figure 3. This involved clamping and aligning the plates before welding with temporary tack welds.

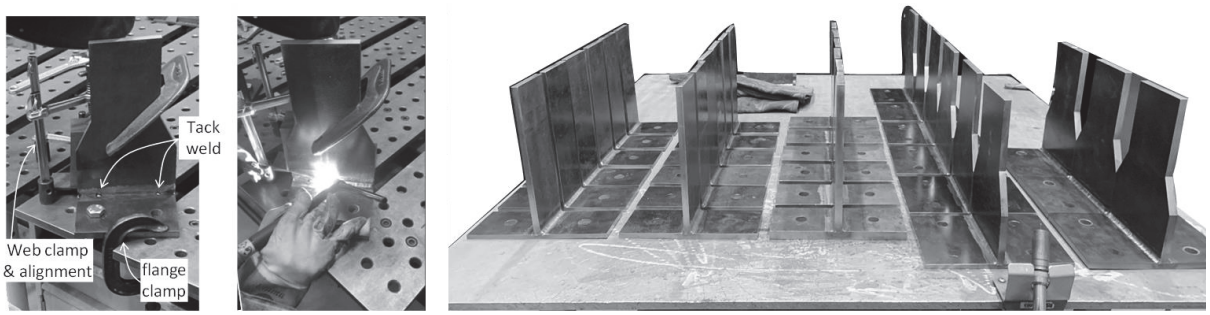

Fig. 3. Test specimens during and after fabrication

Material Properties

Uniaxial monotonic tensile tests were conducted on rectangular coupons extracted from different plate thicknesses. The tests were conducted at different strain rates ranging from 0.002 to 2.0 s^{-1}. For the M16 grade 8.8 bolts, 8mm round coupon specimens were extracted through a turning-down process. Two tests are conducted for each plate thickness at a given strain rate. The average mechanical material properties are summarized in Table 2. This includes the modulus of elasticity (E), the yield stress (f_y), the ultimate stress(f_u), and the fracture-to-gross area ratio (A_f/A_o). Note that f_y represents the lower yield stress, measured at 0.2% strain offset. The reported stress and strain data are based on the engineering response and an extensometer gauge length of 50mm and 25mm for the plate and bolt coupons, respectively.

Table 2. Summary of measured material properties

Plate thickness	Strain rate, $\dot{\varepsilon}$ [s^{-1}]	E [MPa]	f_y [MPa]	f_u [MPa]	ε_u	A_f/A_o
6 mm	0.002	208,079	322	416	0.20	0.28
	0.1	194,835	350	439	0.19	0.33
	0.4	179,608	348	438	0.19	0.32
8 mm	0.002	223,994	341	491	0.15	0.33
	0.1	194,826	363	510	0.15	0.34
	0.4	169.609	379	524	0.14	0.31
	0.8	184,411	393	525	0.14	0.35
10 mm	0.002	202,375	414	525	0.16	0.31
	0.1	207,119	439	541	0.15	0.32
	0.4	190,074	455	555	0.15	0.36
	0.8	172,141	431	541	0.15	0.39

12 mm	0.002	196,212	294	462	0.18	0.29
	0.1	189,957	291	429	0.17	0.30
	0.4	185,229	351	497	0.17	0.31
	0.8	182,903	364	517	0.17	0.31
15 mm	0.002	210,997	248	406	0.22	0.35
	0.1	196,423	296	425	0.19	0.41
	0.4	186,876	315	433	0.19	0.37
	0.8	182,232	286	437	0.20	0.42
	2	180,462	305	442	0.18	0.41
20 mm	0.002	221,041	300	448	0.18	0.34
	0.1	201,604	317	469	0.18	0.34
	0.4	187,810	330	475	0.18	0.35
	0.8	194,083	336	486	0.17	0.34
	2	194,008	333	489	0.17	0.34
M16 Gr 8.8	0.002	197,700	728	914	0.08	0.39
	0.2	171,867	641	821	0.11	0.36
	0.4	158,720	611	821	0.11	0.37

The dependency of the mechanical properties on the strain rate can be visually investigated using the plots in Figure 4. In these plots, a dashed line representing the moving average is superimposed. Also, the mechanical properties in these plots, for each plate thickness, are normalized by the corresponding value at 0.002 s^{-1} to simplify comparison and discussion. Given that the mechanical properties change almost exponentially, the strain rate axis is shown in the logarithmic scale. The observations are consistent with past tests on mild steel materials [14, 29, 30]. Specifically, at $\dot{\varepsilon}$ =0.8 s^{-1}, the yield stress is amplified by 13% on average and up to 25%, compared to the reference pseudo-static 0.002 s^{-1} rate (see Figure 4(a)). Similarly, the ultimate stress is amplified but by a lower factor of 7% (see Figure 4(b)). Up to 15% reduction is observed in the elastic modulus indicating that it is strain-rate sensitive. With respect to material ductility, about 1a 0% increase is observed in the A_f/A_o ratio (see Figure 4(d)), suggesting that the material becomes more brittle at high strain rates. Finally, no notable correlation is observed between all the mechanical properties and the coupon plate thickness; supporting past research observations [29]. For the high-strength grade 8.8 bolt material, different observations are noted where both the yield and ultimate stresses are reduced by about 12% at high strain rates. Others also noted that high-strength steels generally present a less favourable response to the strain rate [29]. The reduction in area at fracture is

about 7% higher at $\dot{\varepsilon}$ = 0.4 s^{-1}, indicating a slightly more ductile response for the bolt at high strain rate. More tests are needed however on bolt components to confirm this observation, since others noted an opposite effect on ductility [14].

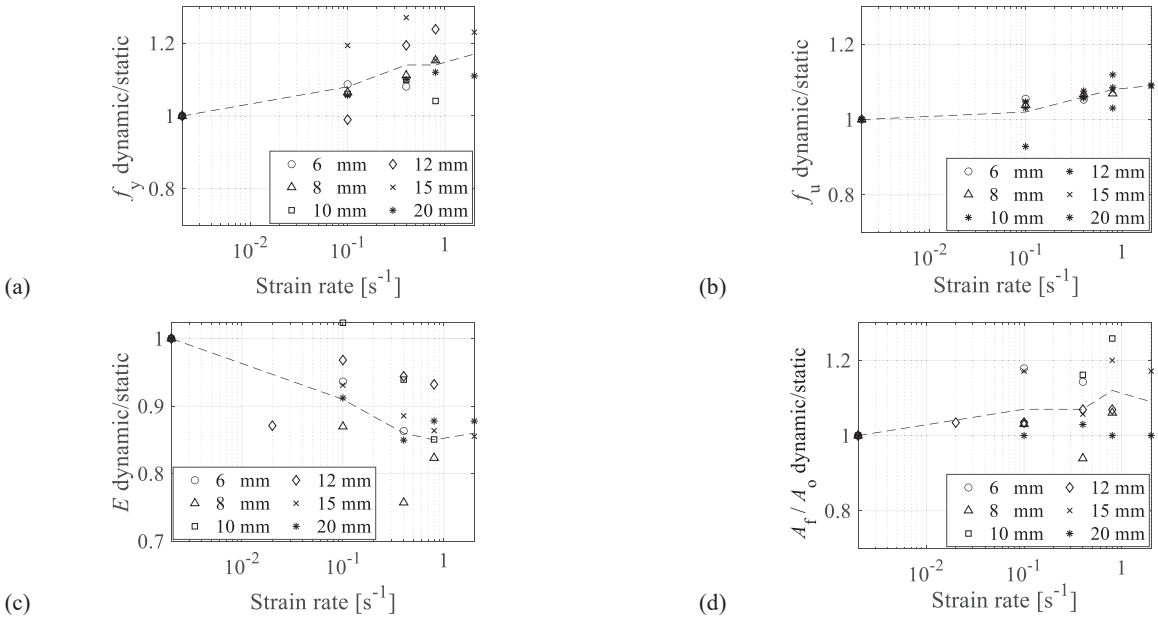

Fig. 4. Normalized mechanical properties for S275 material versus strain rate

Experimental Setup

The tests were conducted in the Testing and Structural Research Laboratory (TSRL) at the University of Southampton, using a 630kN Schenck servo-hydraulic machine, as shown in Figure 5(a). The test specimens were tested in a T-stub to rigid support and double T-stub configurations (see Figure 5(b)). A series of steps were followed in each test. First, the web of the rigid support (or that of the lower T-stub in the case of the double-configuration specimens) is clamped into the machine. The rigid support surface was checked before each test to confirm the absence of distortion and to ensure levelness. Second, the T-stub specimen is centred relative to the rigid support, the bolt holes are aligned and then tightened to the snug-tight or fully preloaded condition. This is done using a gauged torque wrench as shown in Figure 5(c). For the snug-tight condition, the bolts were tightened up to a torque of 80 N.m. For the fully-preloaded condition, a 280N.m torque is used which corresponds to a preload force of about 88kN per

bolt (70% of bolt nominal ultimate tensile resistance), assuming a nut (k) factor equal to 0.20. Full preloading was conducted in two passes (and in a cross pattern in the case of the 4 bolt specimens) to ensure the preload was evenly distributed. Lastly, the T-stub specimen's web is clamped, and tensile loading is applied at the specified loading rate shown in Table 1 up to complete failure. A two-dimensional Digital Image Correlation (DIC) system was employed for all specimens to provide a redundant system for capturing deformations and to investigate the progression of local plastic strains. The DIC measurements were also used to deduce the specimen deformation accurately while omitting any potential slip in the clamps or elastic deformations in the web.

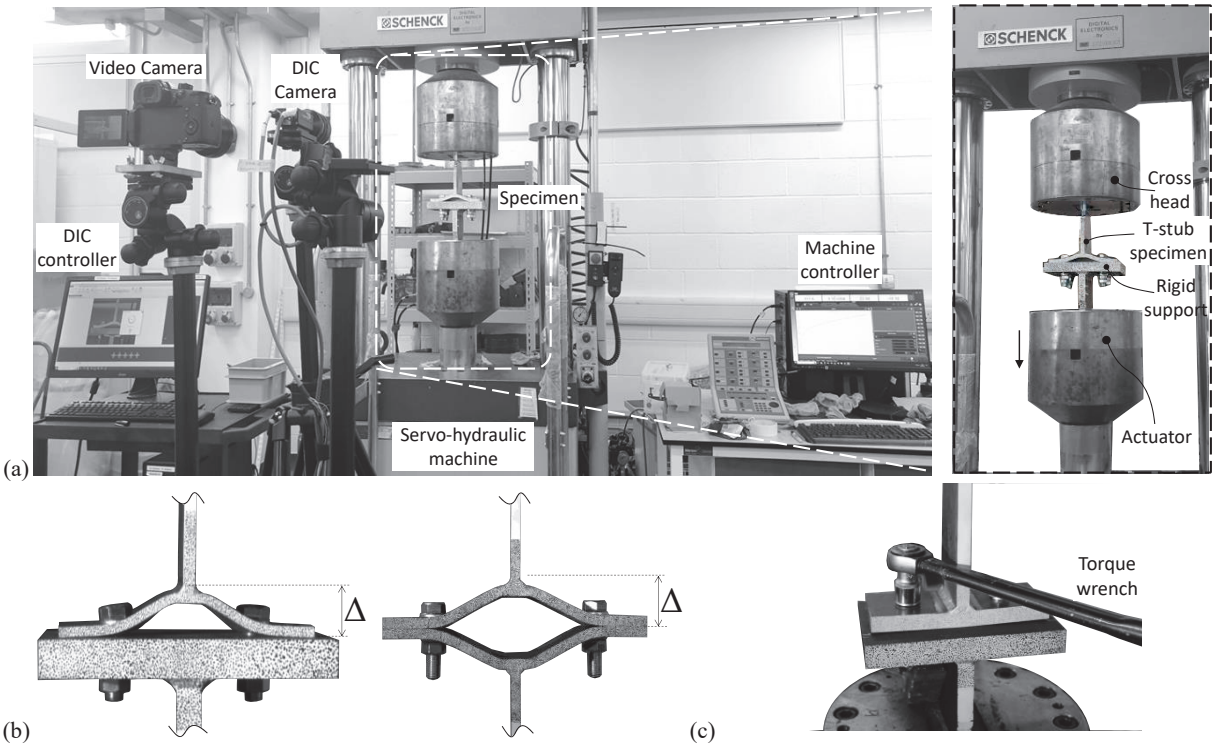

Fig. 5. (a) Test setup for T-stub testing; (b) Specimen types and deformation measurement; (c) Bolt tightening with a torque wrench

Discussion of results

Overall response and deformation modes

The force-deformation curves for all specimens are plotted in Figure 6. To simplify the discussion, a separate figure is provided based on the flange plate thickness and the bolt preload case, in which the

individual responses at the different loading rates are compared. In these plots, The deformation represents the separation gap between the T-stub specimen and the rigid support. In the case of the double T-stub specimens, this deformation represents half of the separation gap (i.e., the deformation of a single T-stub component), as demonstrated in Figure 5(b). For reference, the plastic strength as per Eurocode 3 Part 1-8 [1], $F_{p,\,Rd}$, is computed using the measured pseudo-static material properties and no partial safety factor, and superimposed in the same plots.

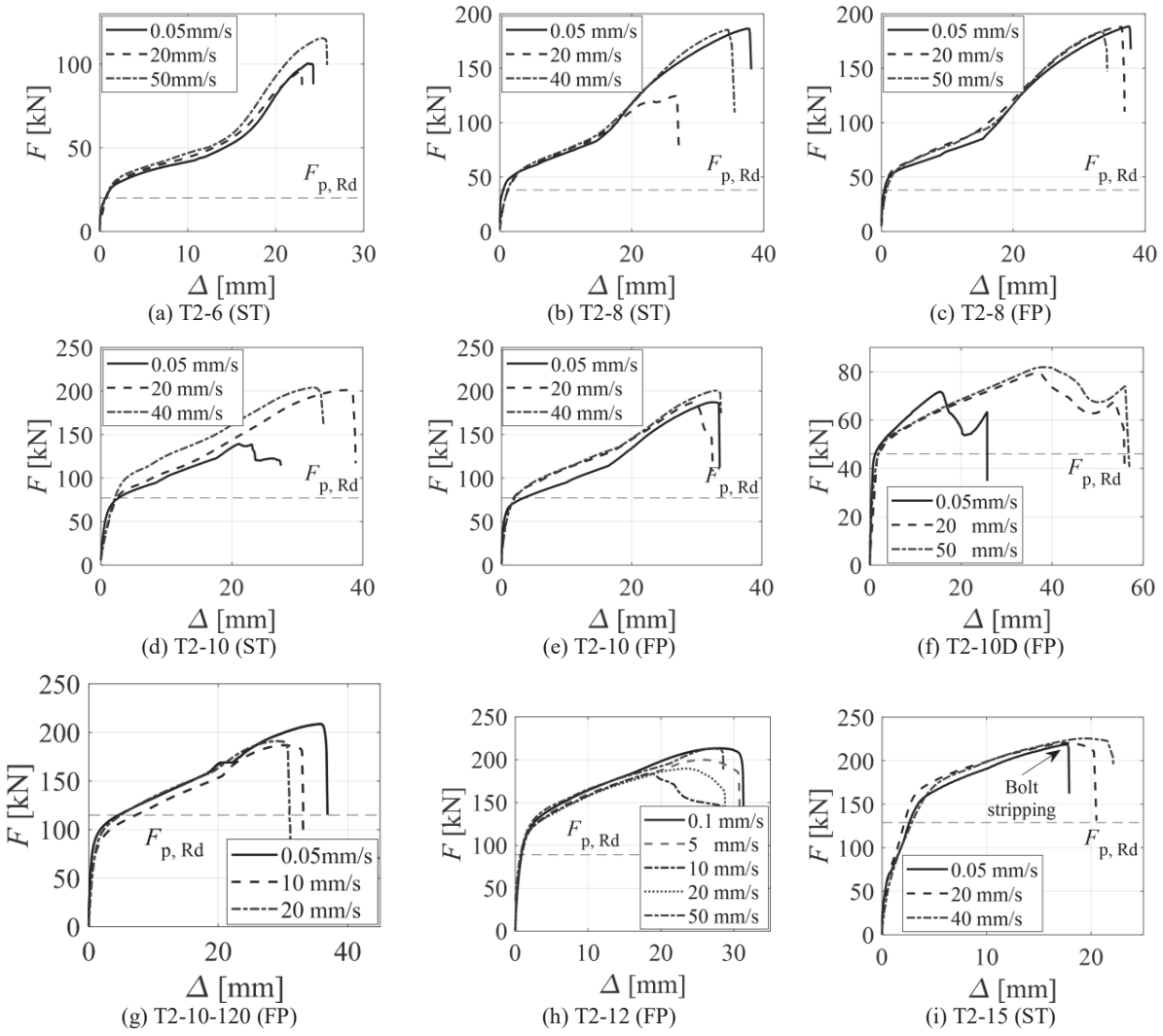

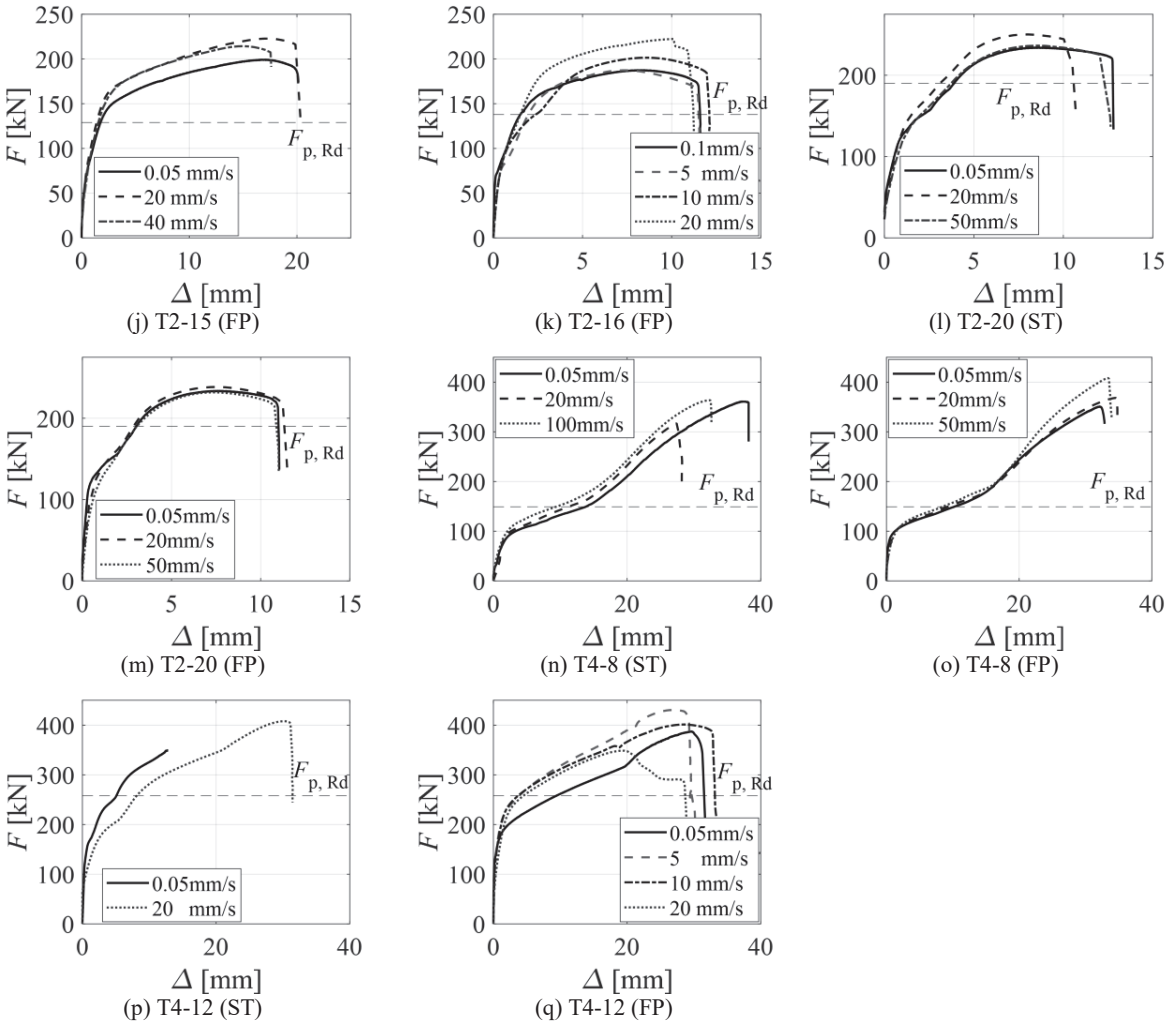

Fig. 6. Distribution of the response parameters based on the collated database: (a) plastic moment, (b) elastic rotational stiffness, and (c) post-yield stiffness

Figure 7(a) shows images of the deformation mode for the two-bolt specimens, with different flange thicknesses, right before failure. The Von Mises equivalent strain contours are superimposed in those images, as computed by the DIC system. The deformation mode depends on the flange plate thickness, as expected. The thin 6mm and 8mm T-stubs are governed by flange bending and bolt-hole elongation (corresponding to *Mode 1* as per CEN [1] classification). The force-deformation response of these specimens is characterized by the onset of the membrane action, evident by the sudden increase in the post-yield slope following flange bending. The membrane action diminishes with thicker 10mm and 12mm flange plates. The thick 15mm to 20mm T-stubs are governed by flange yielding at the weld toe

and bolt elongation (corresponding to *Mode 2* as per CEN [1] classification). Most of the tests failed to bolt rupture as the photo in Figure 7(b) shows. The figure also shows the two types in which bolt rupture manifested: 1) bolt shank rupture under combined shear and tension, and 2) necking followed by bolt thread rupture under tension. The former is observed in thinner specimens while the latter is observed in thicker specimens. Twelve tests failed by weld failure near the weld toes as can be seen in Figure 7(c). This primarily took place in the more flexible T-stub specimens (T2-6-80 and T2-8-80D). The heat-affected zone (HAZ) near the weld toe in those thin/flexible specimens is more prone to failure under larger tensile strains imposed by the membrane action. Only one specimen failed due to bolt thread stripping. This was due to the incorrect usage of the proper nut grade.

To quantitatively evaluate the effect of the bolt preload and loading rate on the T-stub behaviour, response quantities are numerically deduced from the force-deformation data using the procedure described in Elkady [31]. Each response quantity, namely the elastic stiffness, ultimate strength, and ductility, is discussed in the subsequent subsections.

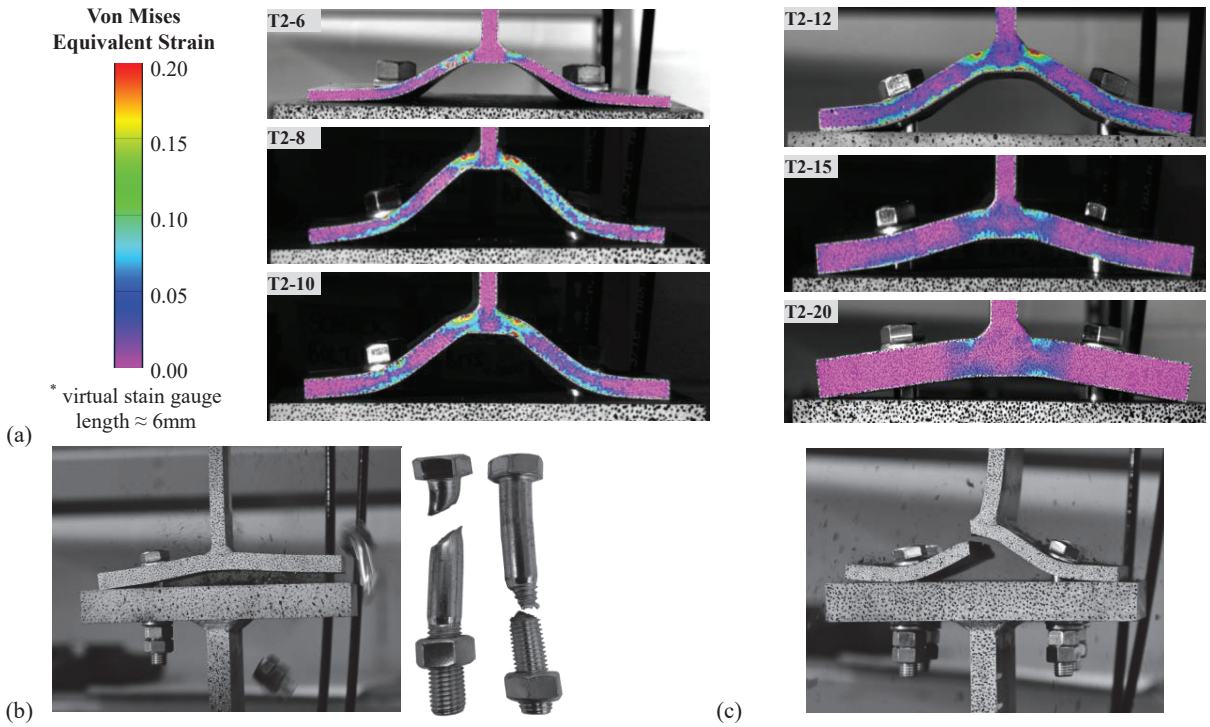

Fig. 7. (a) Deformation modes, right before failure, and corresponding Von Mises strain distribution for 2-bolt T-stubs with different thicknesses; Photos of the observed failure modes: (b) bolt rupture and (c) weld failure

Elastic stiffness

The T-stub elastic stiffness is one of the most fundamental quantities used to quantify the global joint stiffness. This is detrimental in classifying the joint rigidity and in the consequent design process. Figure 8 shows a comparison of the measured elastic stiffness, K_e, for the T-stub specimens. To simplify the visualization and comparison in Figure 8, the stiffness values for each group of T-stub specimens (with the same t_f) are normalized with that of the specimen with pseudo-static loading (i.e., 0.05 mm/s) and snug-tight condition (if applicable). The effect of bolt preload is evident in this plot in all cases. Specimens with fully preloaded bolts develop an elastic stiffness that is, on average, 1.75 times larger than that of a snug-tight specimen. This amplification can be as high as four times, consistent with past observations [18-20]. Generally, the bolt preload will have a lower impact on thin T-stubs, considering that those are controlled by flange bending in double curvature where the prying force is small. One should also note that the absolute value of the stiffness is sensitive to the flange plate's initial imperfection (distortion due to welding) which is more evident in thicker plates [32-35].

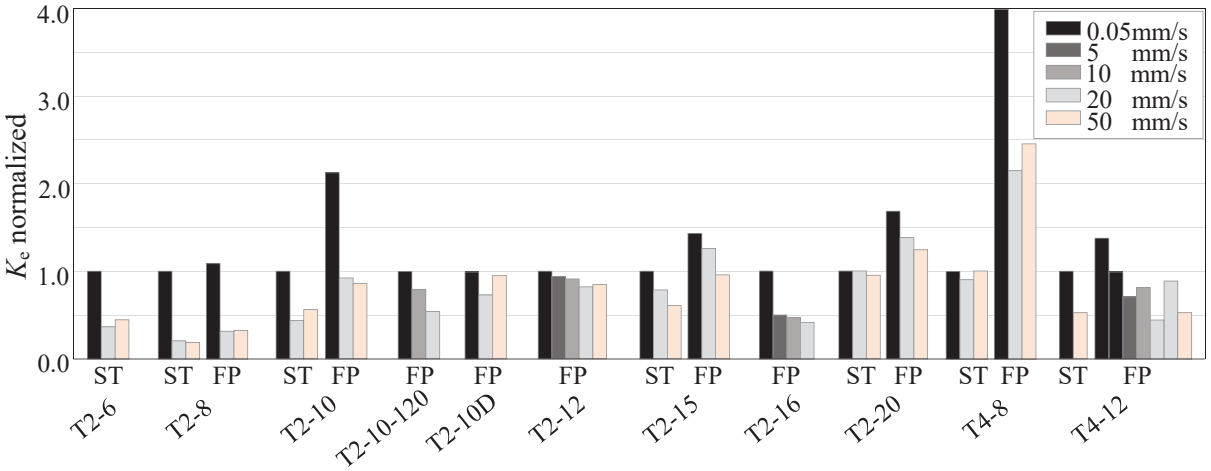

Fig. 8. Comparison of the normalized elastic stiffness

The reduction in the elastic stiffness with higher loading rates is also evident in the bar plot. This is further investigated through Figure 9 which shows K_e, normalized by the pseudo-static K_e, as a function

of t_f. An average of 35% reduction in K_e is observed compared to the 0.05 mm/s case. This is consistent with the reduction level in the elastic modulus that is observed from the material tests. The reduction in stiffness can also be attributed to the loss of -static- friction under high-velocity loading. This is consistent with past research by Suita et al. [2] that noted a 50% drop in friction forces at high loading rates of 4 mm/s. Notwithstanding the uncertainty and sensitivity associated with K_e, A clear trend is also noticeable concerning t_f (refer to the trend line in Figure 9), where the reduction in stiffness under high loading rates is more evident in thinner plates. The reduction in stiffness can be as high as 80% in thin plates. Finally, the preload did not seem to significantly alter the observed loading rate effect. However, in couple of cases (e.g., T2-20 and T4-8), the loading rate effect on stiffness was more pronounced in the preloaded cases. In fully preloaded specimens, static friction is a key feature that reduces slippage and consequently increases stiffness. When this feature is lost under high-speed loading, the drop in stiffness may become pronounced.

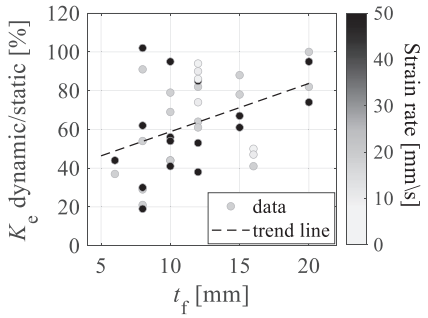

Fig. 9. Relation between reduction in stiffness under high loading rates and the plate thickness

Plastic and Ultimate capacity

Past research mostly reported an increase in the strength of bolted components and joints at high strain rates [24-27]. This is investigated in this section using the deduced ultimate force, F_u. Specimens that failed due to weld failure are excluded from the consequent discussion and computed statistics since those represent premature failure. Referring to Figure 10, the bolt preload condition seems to have no effect on the ultimate capacity of the T-Stub, with an FP-to-ST force ratio ranging between 0.95 to 1.12. The loading rate seems to have a minor effect where an average 5% amplification is observed in F_u. However,

this amplification is inconclusive. That may be due to the reverse effect the strain rate had on the ultimate stress of the plate and bolt materials, as discussed earlier. One should note that similar observations can also be driven about the plastic capacity of the T-Stubs, as inferred from Figure 6.

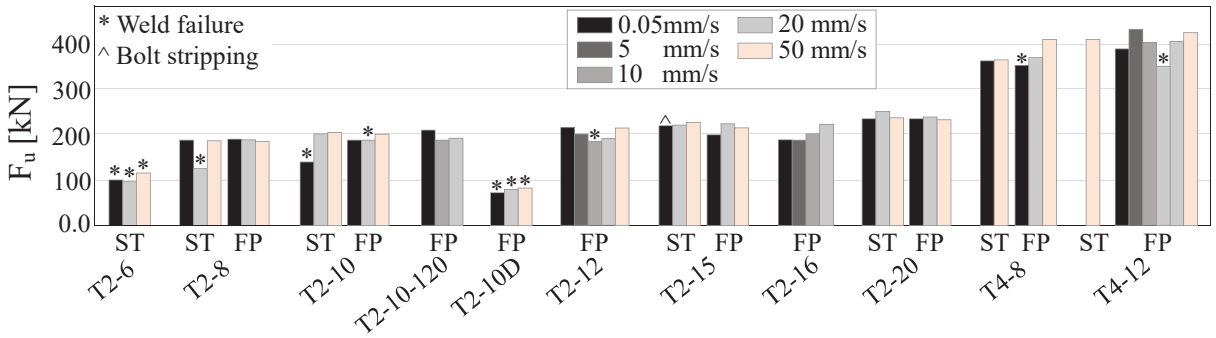

Fig. 10. Comparison of the ultimate capacity

The plastic capacity of the T-stubs is deduced using an equal-area fitting method (refer to [31]). The values are used to assess the plastic design values ($F_{p,Rd}$) predicted by Eurocode 3 Part 1-8 [1]. Figure 11(a) shows the scatter for the test-to-theoretical ratio, where $F_{p,Rd}$ is computed using the pseudo-static material properties. Figure 11(b) is based on $F_{p,Rd}$ which is computed using the actual material properties corresponding to each test loading rate. When using the pseudo-static material properties, the average ratio is about 1.13, indicating that Eurocode 3 will be underestimating the resistance by 13% on average. This is expected given that the material -at least of the plate steel- possesses enhanced strength under high strain rates. If the proper (i.e., loading rate representative) material properties are used, the average ratio drops down to 1.03. This is evident in Figure 11(b) where high loading-rate data points move closer to unity. In design, this can simply be done using prespecified material modification factors. This is critical to avoid altering the damage/failure model stipulated in the design process, particularly in finely tuned bolted joints. It is worth noting that although the prediction error is reduced -on average- in Figure 11(b), it appears that the Eurocode 3 approach tends to underestimate the plastic capacity for thin flange T-stubs by about 40% and overestimate that of thick flange plates by about 35%. This can be attributed to the assumptions used by the Eurocode 3 method, including the discretization of the T-stub deformation shape into three modes, and the idealization of the flange plate yield lines associated with each mode. This type

(and level) of prediction errors is well documented in the literature where several researchers have proposed more accurate variations of this approach [36, 37].

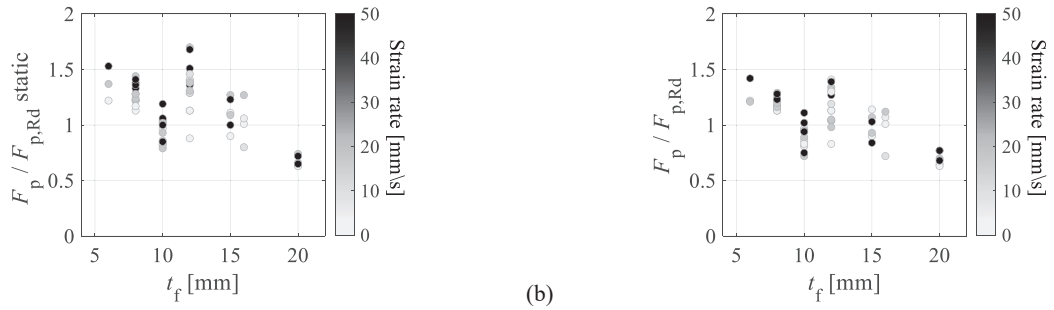

Fig. 11. Measured versus design plastic capacity per [1] versus flange thickness, using (a) pseudo-static material properties, and (b) strain-rate representative material properties

Ductility

The T-stub ductility is quantified using the deformation at failure, Δ_f. As shown in Figure 6, this coincides with the ultimate force (i.e., capping point). The bar plot in Figure 12 compares Δ_f for all tests. As expected from past research, a clear inverse correlation is observed between the specimen ductility and its flange plate thickness. This is already noticeable from the deformation mode in Figure 7. The thin 8mm and 20mm T-stubs deform by about 38mm and 12mm, respectively. Assuming these T-stubs are part of a beam-to-column joint with an extended endplate connection and a 500mm deep beam, this transforms to a joint rotation capacity of 7.6% and 2.4%, respectively. The 8mm T-stub ductility is further amplified by 58% when the bolt gauge length is increased by 50%, from 120mm to 180mm (i.e., specimen T2-10D). The 6mm specimens are excluded from the observed Δ_f-t_f correlation. This is due to the occurrence of significant bolt-hole elongation under increasing membrane forces, which eventually leads to weld failure. No notable difference in ductility between two- and four-bolt specimens of the same thickness.

Excluding specimens failing by weld failure, Figure 12 demonstrates another inverse correlation between ductility and loading rate. At 50 mm/s, ductility appears to be reduced by about 6% to 22%, compared to the pseudo-static 0.05 mm/s loading rate. This effect seems to diminish and become unclear in thick T-stubs with t_f larger than 15mm. This may be attributed to the fact that these plates are more controlled by

bolt tensile elongation and are more affected by other factors such as bolt preload and the initial distortion of the flange plate. Finally, contrary to past research [18], no consistent tendency is observed between ductility improvement and bolt preload across all flange plate thicknesses.

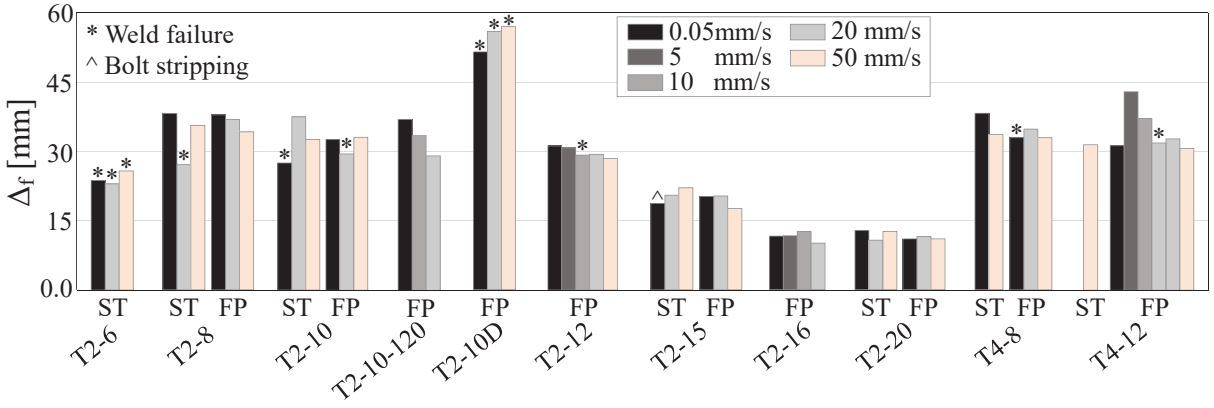

Fig. 11. Comparison of T-stub specimens' deformation at failure

Summary and Conclusions

A total of 57 welded T-stub specimens were tested with different flange plate thicknesses and number of bolt rows. The aim is to generate unique test data for T-stub components, with different preload conditions, undergoing varying loading rates (up to 50 mm/s) that can potentially help in a clearer understanding of high loading/strain rates effects on the mechanical properties of T-stubs. This data addresses the limited number of high-speed/dynamic tests on bolted steel joints/components. The following experimental observations are made:

- Material coupon tests provided consistent findings to those found in the literature. Specifically, for grade S275 steel, the yield and ultimate stresses are amplified on average by 13% and 7%, respectively when subjected to a strain rate of 2 s^{-1}. At the same strain rate, a 15% reduction in the modulus of elasticity. The material also demonstrates brittleness (-10% reduction in ductility) with high strain rates. Opposite observations are made with respect to strength and ductility, for the high-strength grade 8.8 bolt material.

- The T-stubs deformed according to Eurocode 3 *mode 1* and *mode 2*. Thin flange plate (≤8mm) experienced plate bending in double curvature, bolt-hole elongation, and significant membrane action. Thick flange plate (≥15mm) experienced plate yielding near weld toe and bolt elongation followed by bolt tensile rupture. Weld failure was more evident in thin T-stubs and more probable under high loading rates.
- Among the different mechanical properties, the elastic stiffness is the most affected by both the bolt preload and the loading rate. Bolt preload improved the stiffness by up to four times. On the other hand, the stiffness is reduced by about 35% under high loading rates owing to slippage and the reduced materials' elastic modulus. This reduction was more evident in thinner T-stubs.
- The bolt preload did not affect either the plastic or ultimate capacities of the specimens. The loading rate had a rather minor effect. At 50 mm/s, an average 5% increase in the ultimate resistance is observed. This amplification, which is driven by the enhanced material properties, can be as high as 15%. However, there is a notable uncertainty associated with this amplification fact.
- Eurocode 3 Part 1-8 plastic strength prediction can be generally improved if true strain-rate-dependant material properties are used in the computation. Otherwise, the code prediction is on the conservative side by 13% on average. Regardless, a ±40% error is still evident due to the analytical assumptions of the code approach.
- The bolt preload did not affect the T-stub ductility. Conversely, the ductility is shown to be inversely proportional to the loading rate. Failure may occur 22% earlier under higher loading rates. This is more evident in thinner specimens.

Data Availability

The experimental database upon which the current work is based can be made available from the corresponding author upon reasonable request.

Acknowledgements

This work was conducted at the National Infrastructure Laboratory, University of Southampton (UoS). The authors gratefully acknowledge the financial support provided by UoS to the first and second authors as part of their studentship project. The authors would like to thank the Testing and Structures Research Laboratory (TSRL) staff, particularly Aga Murch and Stuart Findlow, for their technical assistance throughout the testing program, as well as former master students Zihan Li and Yan Yan for their support in the first phase of testing.

References

[1] CEN, Eurocode 3 - Design of Steel Structures, Part 1-8: Design of Joints, European Committee for Standardization, Brussels, Belgium, 2005.

[2] K. Suita, K. Kaneta, I. Khozu, The effect of strain rate in steel structural joints due to high speed cyclic reversed loadings, 10th World Conference on Earthquake Engineering, Rotterdam, Netherlands, 1992, pp. 137-145.

[3] P.S.B. Shing, S.A. Mahin, Rate-of-Loading Effects on Pseudodynamic Tests, Journal of Structural Engineering 114(11) (1988) 2403-2420.

[4] D. Forni, B. Chiaia, E. Cadoni, Strain rate behaviour in tension of S355 steel: Base for progressive collapse analysis, Engineering Structures 119 (2016) 164-173.

[5] P. Soroushian, K.-B. Choi, Steel Mechanical Properties at Different Strain Rates, Journal of Structural Engineering 113(4) (1987) 663-672.

[6] A.A. Alabi, P.L. Moore, L.C. Wrobel, J.C. Campbell, W. He, Influence of Loading Rate on the Fracture Toughness of High Strength Structural Steel, Procedia Structural Integrity 13 (2018) 877-885.

[7] C.S. Wiesner, H. MacGillivray, Loading rate effects on tensile properties and fracture toughness of steel, Fracture, Plastic Flow and Structural Integrity, CRC Press2019, pp. 149-174.

[8] K. Wallin, Fracture toughness of engineering materials: Estimation and application, EMAS publishing2011.

[9] D. Dubina, A. Stratan, Behaviour of welded connections of moment resisting frames beam-to-column joints, Engineering Structures 24(11) (2002) 1431-1440.

[10] A. Al-Rifaie, Z.W. Guan, S.W. Jones, Q. Wang, Lateral impact response of end-plate beam-column connections, Engineering Structures 151 (2017) 221-234.

[11] E.L. Grimsmo, A.H. Clausen, M. Langseth, A. Aalberg, An experimental study of static and dynamic behaviour of bolted end-plate joints of steel, International Journal of Impact Engineering 85 (2015) 132-145.

[12] A. Elkady, L. Mak, Data driven evaluation of existing numerical modelling guidelines for semi-rigid connections, 10th International Conference on Behaviour of Steel Structures in Seismic Areas (STESSA), Springer International Publishing, Timisoara, Romania, 2022, pp. 244-251.

[13] Z. Ding, A. Elkady, Semirigid bolted end-plate moment connections: Review and experimental-based assessment of available predictive models, Journal of Structural Engineering 149(9) (2023).

[14] G. Culache, M.P. Byfield, N.S. Ferguson, A. Tyas, Robustness of Beam-to-Column End-Plate Moment Connections with Stainless Steel Bolts Subjected to High Rates of Loading, Journal of Structural Engineering 143(6) (2017) 04017015.

[15] F. Dinu, D. Dubină, I. Marginean, C. Neagu, I. Petran, Structural connections of steel building frames under extreme loading, Advanced Materials Research 1111 (2015) 223-228.

[16] N. Baldassino, M. Bernardi, R. Zandonini, Experimental and numerical analyses of the loading rate influence on the T-stub response, Università degli Studi di Trento, Trento, Italy, 2017, pp. 50-56.

[17] Y. Cai, B. Young, Experimental investigation of carbon steel and stainless steel bolted connections at different strain rates, Steel and Composite Structures 30(6) (2019) 551-565.

[18] Y. Zhang, S. Gao, L. Guo, J. Qu, S. Wang, Ultimate tensile behavior of bolted T-stub connections with preload, Journal of Building Engineering 47 (2022) 103833.

[19] J.-P. Jaspart, R. Maquoi, Effect of bolt preloading on joint behaviour, 1st European Conference on Steel Structures, Athens, Greece, 1995, pp. 219-226.

[20] C. Faella, V. Piluso, G. Rizzano, Experimental analysis of bolted connections: Snug versus preloaded bolts, Journal of Structural Engineering 124(7) (1998) 765-774.

[21] A. Tyas, J.A. Warren, E.P. Stoddart, J.B. Davison, S.J. Tait, Y. Huang, A Methodology for Combined Rotation-Extension Testing of Simple Steel Beam to Column Joints at High Rates of Loading, Experimental Mechanics 52(8) (2012) 1097-1109.

[22] R. Rahbari, A. Tyas, J.B. Davison, E.P. Stoddart, Web shear failure of angle-cleat connections loaded at high rates, Journal of Constructional Steel Research 103 (2014) 37-48.

[23] H. Wang, K.H. Tan, B. Yang, Impact Resistance of Steel Frames with Different Beam-Column Connections Subject to Falling-Floor Impact on Various Locations, Journal of Structural Engineering (United States) 147(4) (2021).

[24] K. Suita, M. Nakashima, K. Morisako, Tests of Welded Beam-Column Subassemblies. II: Detailed Behavior, Journal of Structural Engineering 124(11) (1998) 1245-1252.

[25] K. Udagavva, K. Takanashi, B. Kato, Effects of displacement rates on the behavior of steel beams and composite beams, 8th World Conference on Earthquake Engineering, San Francisco, CA, USA, 1984, pp. 177-184.

[26] A. El Hassouni, A. Plumier, A. Cherrabi, Experimental and numerical analysis of the strain-rate effect on fully welded connections, Journal of Constructional Steel Research 67(3) (2011) 533-546.

[27] Y. Chen, J. Huo, W. Chen, H. Hao, A.Y. Elghazouli, Experimental and numerical assessment of welded steel beam-column connections under impact loading, Journal of Constructional Steel Research 175 (2020) 106368.

[28] ISO 4014, Fasteners – Hexagon head bolts – Product grades A and B, DIN 931/EN ISO 4014: 2022-10, International Organization for Standardization, Geneva, Switzerland, 2022.

[29] M.F.D.F. Pereira, Robustness of multi-storey steel-composite buildings under column loss: rate-sensitivity and probabilistic framework, Department of Civil and Environmental Engineering, Imperial College London, London, UK, 2012.

[30] K. Kawata, A new testing method for the characterization of materials in high velocity tension, Mechanical Properties at High Rates of Strain 1979 (1979) 71-80.

[31] A. Elkady, Response characteristics of flush end-plate connections, Engineering Structures 269 (2022).

[32] O. Yapici, Advanced finite element modelling of stainless steel bolted T-stubs under large deformations, Structures 58 (2023) 105461.

[33] R. Tartaglia, M. D'Aniello, M. Zimbru, Experimental and numerical study on the T-Stub behaviour with preloaded bolts under large deformations, Structures 27 (2020) 2137-2155.

[34] A.P. Mann, L.J. Morris, Significance of Lack of Fit-Flush Beam-Column Connections, Joints in structural steelwork, Pentech Press, London, 1981, pp. 6.22-6.36.

[35] T. Mineyama, Research on rationalization of bridge member connection structure using high-strength bolt tensile joints (in Japanese), Graduate School of Engineering, Osaka City University, Osaka, Japan, 2020.

[36] A.M.G. Coelho, Characterization of the ductility of bolted end plate beam-to-column steel connections, Department of Civil

Engineering, University of Coimbra, Coimbra, Portugal, 2004.

[37] A.C. Faralli, M. Latour, P.J. Tan, G. Rizzano, P. Wrobel, Experimental investigation and modelling of T-stubs undergoing large displacements, Journal of Constructional Steel Research 180 (2021) 106580.